NATIONAL ADVISORY COMMITTEE
FOR AERONAUTICS

TECHNICAL NOTE

No. 1729

FLIGHT DETERMINATION OF WING AND TAIL LOADS ON A FIGHTER-

TYPE AIRPLANE BY MEANS OF STRAIN-GAGE MEASUREMENTS

By William S. Aiken, Jr.

Langley Aeronautical Laboratory
Langley Field, Va.

Washington

October 1948

NATIONAL ADVISORY COMMITTEE FOR AERONAUⱢᵢᵤᵤ

TECHNICAL NOTE NO. 1729

FLIGHT DETERMINATION OF WING AND TAIL LOADS ON A FIGHTER-

TYPE AIRPLANE BY MEANS OF STRAIN-GAGE MEASUREMENTS

By William S. Aiken, Jr.

SUMMARY

A flight investigation was conducted to determine the contributions of wing, tail, and fuselage to the total airplane lift of a propeller-driven fighter-type airplane. The tests covered a Mach number range from 0.2 to 0.8. The loads on the various airplane components were measured by the use of calibrated strain-gage installations located at the roots of the wings and horizontal tail surfaces.

The results of the investigation showed that the center of pressure of the wing additional air load remained constant near the lifting-line-theory value up to the highest Mach number (0.8) attained in the tests. The fuselage load per unit normal acceleration appeared to be unaffected by Mach number changes. Adequate correlation was obtained between various tail-load parameters derived from the flight-test results and from wind-tunnel tests. Strain-gage measurements have been found to offer an accurate and convenient method for determining loads in flight.

INTRODUCTION

Although there are numerous wind-tunnel tests of airfoils and airplane models available at speeds which extend into the transonic range, the flight-loads data available for correlation are not only meager but for the most part are confined to relatively low Mach numbers. In order to obtain flight-loads data at high subsonic speeds, the National Advisory Committee for Aeronautics investigated a specially reinforced fighter-type airplane for the purpose of determining buffeting and transient loads. Some results of the buffeting tests have been published in reference 1. The strain-gage instrumentation used in the buffeting tests was adequate for the evaluation of wing additional-air-load center of pressure,

fuselage load per unit normal acceleration, wing-fuselage zero-lift
pitching-moment coefficient, wing-fuselage aerodynamic center, and
tail loads due to angular acceleration in pitch below the buffeting
boundary. The purposes of this paper are to present the results
of the flight investigations below the buffeting boundary and to
indicate the correlation existing between the quantities mentioned
and the wind-tunnel-test results or theoretical calculations, or
both.

SYMBOLS

B	aerodynamic bending moment, inch-pounds
S_h	aerodynamic shear, pounds
F	fuselage load, pounds
y_{cp}	spanwise distance of aerodynamic center of pressure from reference station, inches
M	Mach number
q	dynamic pressure, pounds per square foot
W	airplane weight, pounds
I_Y	airplane moment of inertia in pitch, slug-feet square
k_Y	radius of gyration in pitch, feet
S	wing area, square feet
n	airplane normal acceleration at center of gravity (measured perpendicular to thrust line), g units
g	acceleration due to gravity, feet per second per second
C_N	airplane normal-force coefficient $\left(\dfrac{nW}{qS}\right)$
L_t	horizontal-tail load, pounds
$L_{t_{\ddot{\theta}}}$	portion of horizontal-tail load associated with pitching acceleration, pounds
C_{m_0}	pitching-moment coefficient of wing-fuselage combination at zero lift and $M = 0$

c_{m_0} wing section pitching-moment coefficient at zero lift

$\bar{c}$ mean aerodynamic chord, feet

x_t distance from wing-fuselage aerodynamic center to
             horizontal-tail center of pressure, positive
             forward, feet

x distance from airplane center of gravity to wing-
           fuselage aerodynamic center, positive forward, feet

$l_t = x_t - x$

$\ddot{\theta}$ angular acceleration in pitch, radians per second
                       per second

y lateral distance from airplane center line, feet

b wing span, feet

Subscripts:

a   additional air load

q   function of dynamic pressure

L   left wing

R   right wing

APPARATUS AND TESTS

Airplane

The airplane used in these tests was of conventional external appearance; however, the horizontal tail, fuselage, wing, canopy, and cowling had been heavily reinforced to provide an extra safety margin against structural failure in the investigation of buffeting loads. Pertinent geometric characteristics of the airplane are given in a three-view diagram, figure 1, and in table I.

Instrumentation

Standard NACA recording instruments were used to record time histories of impact pressure; pressure altitude; normal, longitudinal, and lateral center-of-gravity accelerations; right and left aileron and elevator positions; rate of pitch; and elevator and aileron stick forces. A mechanical timer was used to correlate data from all recording instruments.

The airspeed head was mounted on a boom extending 1.2 local chords ahead of the leading edge of the right wing tip. The NACA airspeed-altitude recorder was located in the right wing to minimize any lag effects. The entire airspeed system was calibrated for position error up to a Mach number of 0.78.

Normal accelerations at the center line of the horizontal tail were measured by means of a strain-gage-type accelerometer and recorded by a multiple recording oscillograph.

The strains at various parts of the wing and horizontal tail structure were measured with wire-resistance strain gages connected as four-arm bridges and recorded by a multiple recording oscillograph. Strain-gage bridges on the shear webs of wing and stabilizer spars were used to measure shear strains; strain-gage bridges on the spar flanges were used to measure bending strains. The strain-gage bridges were mounted at the 30-inch $\left(\dfrac{y}{b/2} = 0.135\right)$ and 35-inch $\left(\dfrac{y}{b/2} = 0.158\right)$ semispan stations on the right and left wings, respectively, and at the 9-inch semispan stations on the left and right stabilizers. In order to obtain calibrations for the conversion of measured strains into bending moments and shears, tests were carried out in the Langley aircraft loads calibration laboratory. The scope of the calibrations was such that the following accuracies for loads measurements could be estimated:

Wing shears, pounds per side. . . . . ±200
Wing bending moments, inch-pounds per side. . . . . ±10,000
Total horizontal-tail shear, pounds . . . . ±50

Tests

The tests reported herein all apply to load-factor conditions within the V-n envelope where no buffeting occurred. The data presented were obtained during flight at altitudes ranging from 5,000 feet to 30,000 feet. In these tests the wing shears and bending moments were measured in either abrupt pull-ups to just below the stall or in a piloting sequence consisting of a rapid push-down followed by a rapid pull-up. An attempt was made to hold the Mach number constant and the ailerons neutral during these maneuvers. The average variation of Mach number in a given run was about $\pm\frac{1}{2}$ percent.

Maneuvering tail loads were determined in slow turns as well as in the push-down - pull-up maneuvers.

All flight tests were made with the airplane in the clean condition, with normal rated power, and with the center of gravity located at 25.1 percent mean aerodynamic chord.

RESULTS AND DISCUSSION

Spanwise Center of Pressure of Wing Load

On the basis of experience the lift or load distribution over a wing is usually considered to consist of two main components. One component, the basic distribution, consists of the distribution with a net lift of zero and is caused by geometric and elastic twist $\left(\text{due to } c_{m_0}\right)$, aileron deflection, and rate of roll. This basic distribution is independent of angle of attack or normal-force coefficient. The other component, termed the "additional distribution," depends only on the angle of attack or normal-force coefficient at a given Mach number and dynamic pressure.

With the load divided as stated, the bending moment at the wing root may be expressed by two terms as follows:

$$B = B_q + B_a$$

where B_a is obtained from the equation

$$B_a = \frac{dB}{dS_h} S_h$$

so that

$$B = B_q + y_{cp_a} S_h$$

In the foregoing equations the subscript q refers to the bending-moment increment due to the basic air load, which varies with dynamic pressure, and the subscript a refers to the additional air loads.

If during a given maneuver the dynamic pressure and the twist characteristics - that is, the twist, aileron deflection, and rate of roll - remain constant, then the center of pressure of the additional air load can be determined from the slope of the curve of bending moment plotted against shear.

Flight-test results.- In the flight tests, results from 34 abrupt push-down and pull-up maneuvers were available in which the left- and right-wing loads were measured at pressure altitudes from 5,000 feet to 30,000 feet and at Mach numbers from 0.2 to 0.8. The maneuvers

covered a normal-force-coefficient range from -0.66 to 1.25. A
typical maneuver illustrating the type of data available for analysis
is shown in figure 2 for an abrupt push-down - pull-up maneuver
executed at 10,000 feet. It will be noted in this figure that the
Mach number is reasonably constant throughout the maneuver because
the maneuver was abrupt. There was less than a 100-foot change in
pressure altitude.

The strain gages measure a structural load, that is, an aero-
dynamic load plus an inertia load; therefore, acceleration data
were used to correct the measured loads for inertia effects by
simply adding values of the wing weight multiplied by $n - 1$ to
the shear measurements outboard of the strain-gage measuring station.
A similar correction was applied to bending-moment results. Now,
as stated previously, if the dynamic pressure remains constant during
a maneuver, the center of pressure of the additional air load is
determined by taking the slope of the curve of bending moment plotted
against shear. The aerodynamic bending moments for the left and right
wings are plotted against the corresponding aerodynamic shears in
figure 3 for the maneuver illustrated in figure 2. The slope of each
line was found by a least-squares method and the centers of pressure
thus determined were 75.9 inches for the left wing and 79.8 inches
for the right wing. These centers of pressure are for the load outboard
of the strain-gage semispan station, but an approximate check indicates
that the centers of pressure for these loads on each wing are roughly
at the same spanwise location as follows:

$$y_{cp_L} = 75.9 + 35 = 110.9 \text{ inches}$$
$$y_{cp_R} = 79.8 + 30 = 109.8 \text{ inches}$$

The procedure outlined was followed for all the maneuvers
considered and the results, in terms of the center of pressure of the
additional air load outboard of the strain-gage station, are given
in figure 4 as a function of Mach number. The theoretical rigid-wing
additional-air-load centers of pressure for the test airplane were
computed by lifting-line and strip theories and are shown in figure 4
as the solid and dashed lines, respectively. The experimental data
show no trend for these centers of pressure to move either outboard
or inboard with Mach number but rather tend to scatter about the line
predicted by lifting-line theory. Sixty percent of the points shown
in figure 4 represent deviations from lifting-line-theory values of
less than the probable error associated with the determination of the
experimental center of pressure. The average probable error for all
points shown is ±1.63 inches.

Wind-tunnel results.- An analysis of data from pressure-distribution
measurements made on a $\frac{1}{3}$-scale model of a prototype of the test airplane

was made to determine the variation of additional-air-load center of pressure with Mach number. The wing plan forms and aerodynamic characteristics of the model and the test airplane were essentially the same. Pressure distributions were measured at semispan station $\frac{y}{b/2}$ equal to 0.211, 0.511, 0.673, 0.839, and 0.935. The tests were conducted in the Ames 16-foot high-speed wind tunnel to find the effect of aileron deflection on span loading. The additional-air-load centers of pressure for the model were calculated by using points at various normal-force coefficients at a constant Mach number and then determining the slopes of the curves of bending moment plotted against shear. The results are shown in figure 5 for aileron angles of 9° and -9°. It should be remembered that the additional air load is independent of aileron angle. The centers of pressure are expressed in terms of the dimensions for the full-size airplane. There is an apparent outboard movement of the center of pressure in the Mach number range from 0.70 to 0.80, but this trend is not evident from flight-test results (fig. 4) and is somewhat questionable when the scatter of the data at constant Mach number for the two different aileron angles is considered, since the additional-air-load center of pressure is independent of aileron angle. The discrepancy may be due to differences in elastic characteristics of the model wing and the airplane wing.

Flight data from pressure-distribution measurements on two airplanes.- Although flight data on wing span loading are generally meager, tests on two airplanes (references 2 and 3) furnished a limited amount of data from which the additional-air-load center of pressure could be computed. The variation of additional-air-load center of pressure with Mach number is shown in figure 6(a) for the airplane of reference 2 and in figure 6(b) for the airplane of reference 3. For the airplane in figure 6(a) there is a trend toward inboard movement of the center of pressure with increasing Mach number, but considerable error is possible in the determination of the points at $M = 0.70$ and $M = 0.78$ since only two airplane normal-force coefficients were available for the computation of the center of pressure. The data of figure 6(b) show no change in center of pressure with Mach number. The results shown in figures 4 to 6, in general, indicate that the additional-air-load center of pressure of an unstalled unswept wing may be expected to remain constant up to a Mach number of 0.85 and to be in good agreement with the lifting-line-theory values.

Fuselage Loads

The determination of fuselage loads by using strain-gage measurements as has been done in the case of the test airplane is relatively simple.

If\the normal acceleration, the airplane weight, the horizontal-tail load, and the left- and the right-wing shears are known at all times, the fuselage load can be found from the equation

$$F = nW - \left(S_{h_L} + S_{h_R} + L_t\right)$$

The fuselage load thus includes the small portion of the wing area inboard of the strain-gage stations. In order to determine the variation of fuselage load with Mach number, the push-down - pull-up maneuvers described previously were used. The fuselage load F was plotted against the normal acceleration; the slope of this line $\frac{dF}{dn}$ is the fuselage load per unit normal acceleration for a particular Mach number. A typical variation of fuselage load with normal acceleration is illustrated in figure 7 for a Mach number of 0.51 at a pressure altitude of 20,000 feet. The fuselage load per unit normal acceleration found from curves of this type is plotted in figure 8 as a function of Mach number. A theoretical value (1713 lb/g), computed by assuming that the load carried by the fuselage was equivalent to the load on the wing area inboard of the strain-gage stations and through the fuselage, passes approximately through the center of the data. No apparent variation of fuselage load with Mach number may be noted.

Horizontal-Tail Loads

The aerodynamic tail load may be expressed as

$$L_t = -C_{m_0} \frac{1}{\sqrt{1 - M^2}} \frac{qS\bar{c}}{x_t} + \frac{nWx}{x_t} + \frac{I_Y\ddot{\theta}}{x_t} \tag{1}$$

The factor $1/\sqrt{1 - M^2}$ is introduced in this equation because the C_{m_0}-term cannot otherwise be determined. The Mach number range is limited to 0.8, and in this range the Glauert factor should be adequate. In order to supplement data obtained in high-speed dives a series of very slow turns were made in which $\dot{\theta}$ was approximately equal to zero. Equation (1) may then be written as

$$\frac{L_t}{q/\sqrt{1 - M^2}} = -C_{m_0} \frac{S\bar{c}}{x_t} + \frac{n}{q} \frac{Wx\sqrt{1 - M^2}}{x_t}$$

or

$$\frac{L_t}{q/\sqrt{1 - M^2}} = -C_{m_0} \frac{S\bar{c}}{x_t} + C_N \frac{Sx\sqrt{1 - M^2}}{x_t}$$

The measured values of $\dfrac{L_t}{q/\sqrt{1 - M^2}}$ in the Mach number range from

0.2 to 0.8 were plotted against $C_N\sqrt{1 - M^2}$ as shown in figure 9. The data of figure 9 are for an airplane weight of 8750 pounds and a center-of-gravity position of 25.1 percent mean aerodynamic chord. The relative lack of scatter for this data justifies the inclusion of the Glauert factor. A curve faired through this data is linear up to a normal-force coefficient of about 0.5. In this linear region the aerodynamic-center position x may be determined from the slope of the curve as

$$\frac{d\left(\dfrac{L_t}{q/\sqrt{1 - M^2}}\right)}{d\left(C_N\sqrt{1 - M^2}\right)} = \frac{Sx}{x_t} = \frac{Sx}{l_t + x}$$

With x determined, C_{m_0} may be found from the intercept of the curve at $C_N\sqrt{1 - M^2} = 0$ as

$$C_{m_0} = - \frac{l_t + x}{S\bar{c}} \frac{L_t}{q/\sqrt{1 - M^2}}$$

The variation of the quantity $\dfrac{L_t}{q/\sqrt{1 - M^2}}$ with $C_N\sqrt{1 - M^2}$, as determined

from tests of a $\frac{1}{3}$-scale model of an airplane (reference 4) with the same basic design as the airplane shown in figure 1, is shown in figure 9. The agreement in the lower normal-force-coefficient range

is considered good. In table II are listed the tail-load parameters which may be derived from the curves shown in figure 9. The agreement between the low-speed values of C_{m_0} for the flight-test results and wind-tunnel results is excellent as is the agreement between the tail-off aerodynamic-center position x and the tail load per unit normal acceleration at low values of $C_N\sqrt{1 - M^2}$ for both flight and wind-tunnel results. The values of tail load per unit normal acceleration listed in table II apply only at the listed values of $C_N\sqrt{1 - M^2}$, since actual tail loads would have to be determined by an integration process at values of $C_N\sqrt{1 - M^2}$ above 0.4.

The variation of the aerodynamic-center position in percent of the mean aerodynamic chord from the leading edge is given in figure 10 as a function of $C_N\sqrt{1 - M^2}$ for the test airplane. The values in this figure were obtained from the slope of the line through the experimental points in figure 9. The tail-off aerodynamic center shifted forward with increase in airplane normal-force coefficient.

The determination of aerodynamic tail loads due to angular acceleration in pitch must be accomplished indirectly by subtracting calculated values of balancing tail load from measured tail loads and plotting the resulting differences against airplane angular acceleration. The results of these computations made for several abrupt push-down - pull-up maneuvers are shown in figure 11. The angular accelerations were determined from normal-acceleration measurements at the center of gravity and the tail of the test airplane. The theoretical values of $L_{t_{\ddot{\theta}}}$ were calculated from the expression

$$L_{t_{\ddot{\theta}}} = \frac{Wk_Y^2}{gx_t}\,\ddot{\theta}$$

where W equals 8750 pounds, k_Y equals 5.5 feet, g equals 32.2 feet per second per second, and x_t equals -16.78 feet. For these values $\dfrac{dL_{t_{\ddot{\theta}}}}{d\ddot{\theta}}$ equals -490 pounds per radian per second per second. The agreement of the experimental values with the calculated values is considered adequate since the determination of the experimental values required the use of small differences of large numbers.

CONCLUSIONS

From the results of the flight tests and correlation with some wind-tunnel-test results, the following conclusions were indicated:

1. The results of the determination of wing additional-air-load center of pressure from strain-gage measurements of root bending moments and shears for the test airplane indicated good agreement with lifting-line theory and showed that the center of pressure of the additional air load might be expected to remain constant up to a Mach number of 0.8.

2. A comparison of wind-tunnel additional-air-load center-of-pressure results for a model of a prototype of the test airplane with flight results showed that the outboard shift of load predicted from wind-tunnel tests was not evident in flight.

3. With the data determined from flight pressure-distribution measurements on the airplanes of NACA ARR No. 4K09 and NACA TN No. 1181, it appeared that the additional-air-load center of pressure might remain constant to Mach numbers of 0.85.

4. The fuselage load per unit normal acceleration for the test airplane remained approximately constant in the Mach number range of the tests with the data tending to scatter about a theoretical value which was computed by assuming that the load carried by the fuselage was equivalent to the load on the wing area inboard of the strain-gage stations and through the fuselage.

5. The tail-load measurements for the test airplane showed excellent agreement between flight and wind-tunnel values of the zero-lift pitching-moment coefficient and between flight and wind-tunnel values of the tail-off aerodynamic-center position at low airplane normal-force coefficients.

6. Flight tail-load measurements indicated that as the airplane normal-force coefficient increased there was a forward shift in the tail-off aerodynamic-center position.

7. Values of tail loads due to angular accelerations in pitch derived from flight measurements gave reasonable agreement with calculated values.

8. Because of the agreement between the flight measurements and wind-tunnel or theoretical results, the use of properly calibrated strain-gage installations to measure wing and tail loads offered an accurate and convenient means of determining over-all loads in flight.

Langley Aeronautical Laboratory
    National Advisory Committee for Aeronautics
        Langley Field, Va., August 13, 1948

REFERENCES

1. Stokke, Allen R., and Aiken, William S., Jr.: Flight Measurements of Buffeting Tail Loads. NACA TN No. 1719, 1948.

2. Clousing, Lawrence A., Turner, William N., and Rolls, L. Stewart: Measurements in Flight of the Pressure Distribution on the Right Wing of a P-39N-1 Airplane at Several Values of Mach Number. NACA ARR No. 4K09, 1945.

3. Brown, Harvey H., and Clousing, Lawrence A.: Wing Pressure-Distribution Measurements up to 0.866 Mach Number in Flight on a Jet-Propelled Airplane. NACA TN No. 1181, 1947.

4. Hall, Charles F.: The Effect of Modifications to the Horizontal-Tail Profile on the High-Speed Longitudinal Control of a Pursuit Airplane. NACA TN No. 1302, 1947.

TABLE I

CHARACTERISTICS OF AIRPLANE

Wing:
   Span, ft 37.03
   Area, sq ft 240.1
   Mean aerodynamic chord, ft 6.63
   Airfoil. . . . . Low drag
   Aspect ratio 5.7

Horizontal tail:
   Span, ft 13.18
   Area, sq ft 41.0
   Incidence, deg 1

Weight during tests, lb 8750

Center-of-gravity position during tests,
   percent M.A.C. 25.1

Approximate radius of gyration in pitch, ft 5.5

Tail length, l_t, ft . . . . -15.84

TABLE II

COMPARISON OF FLIGHT AND WIND-TUNNEL TAIL-LOAD PARAMETERS

[Center of gravity at 25.1 percent M.A.C.; W = 8750 lb]

Tail-load parameter	Flight results	Wind-tunnel results from reference 4
Zero-lift tail-off pitching-moment coefficient, C_{m_0}	-0.0520	-0.0528
Tail-off aerodynamic-center position, distance from center of gravity to aerodynamic center, x, percent M.A.C.:		
At $C_N\sqrt{1 - M^2}$ = 0 to 0.4	-10.98	-10.60
At $C_N\sqrt{1 - M^2}$ = 0.5	-11.25	-10.60
At $C_N\sqrt{1 - M^2}$ = 0.7	-13.17	-10.60
At $C_N\sqrt{1 - M^2}$ = 0.9	-25.10	-10.60
Tail load per unit normal acceleration, lb/g:		
At $C_N\sqrt{1 - M^2}$ = 0 to 0.4	380	367
At $C_N\sqrt{1 - M^2}$ = 0.5	389	367
At $C_N\sqrt{1 - M^2}$ = 0.7	450	367
At $C_N\sqrt{1 - M^2}$ = 0.9	702	367
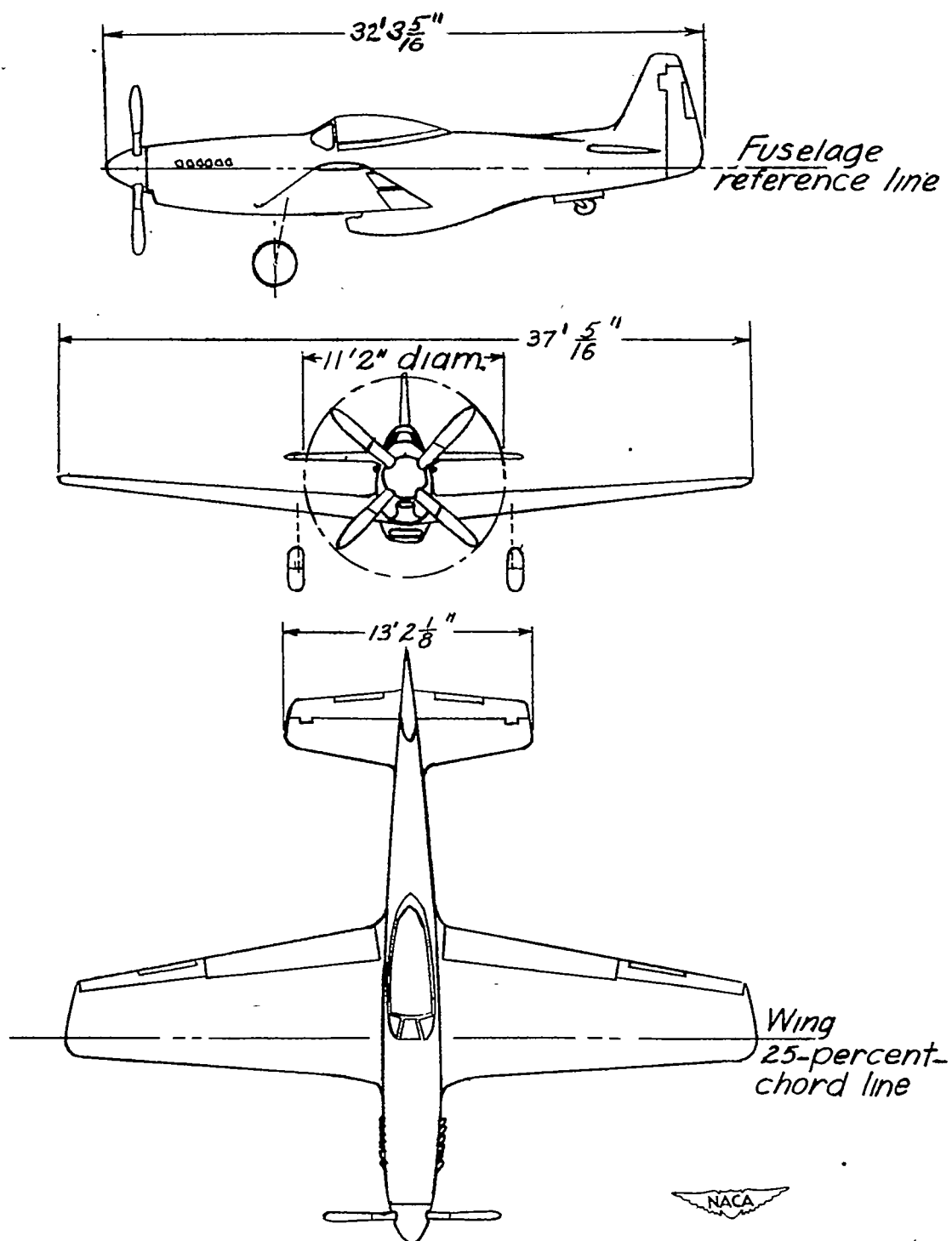
Figure 1.— Three-view diagram of test airplane.
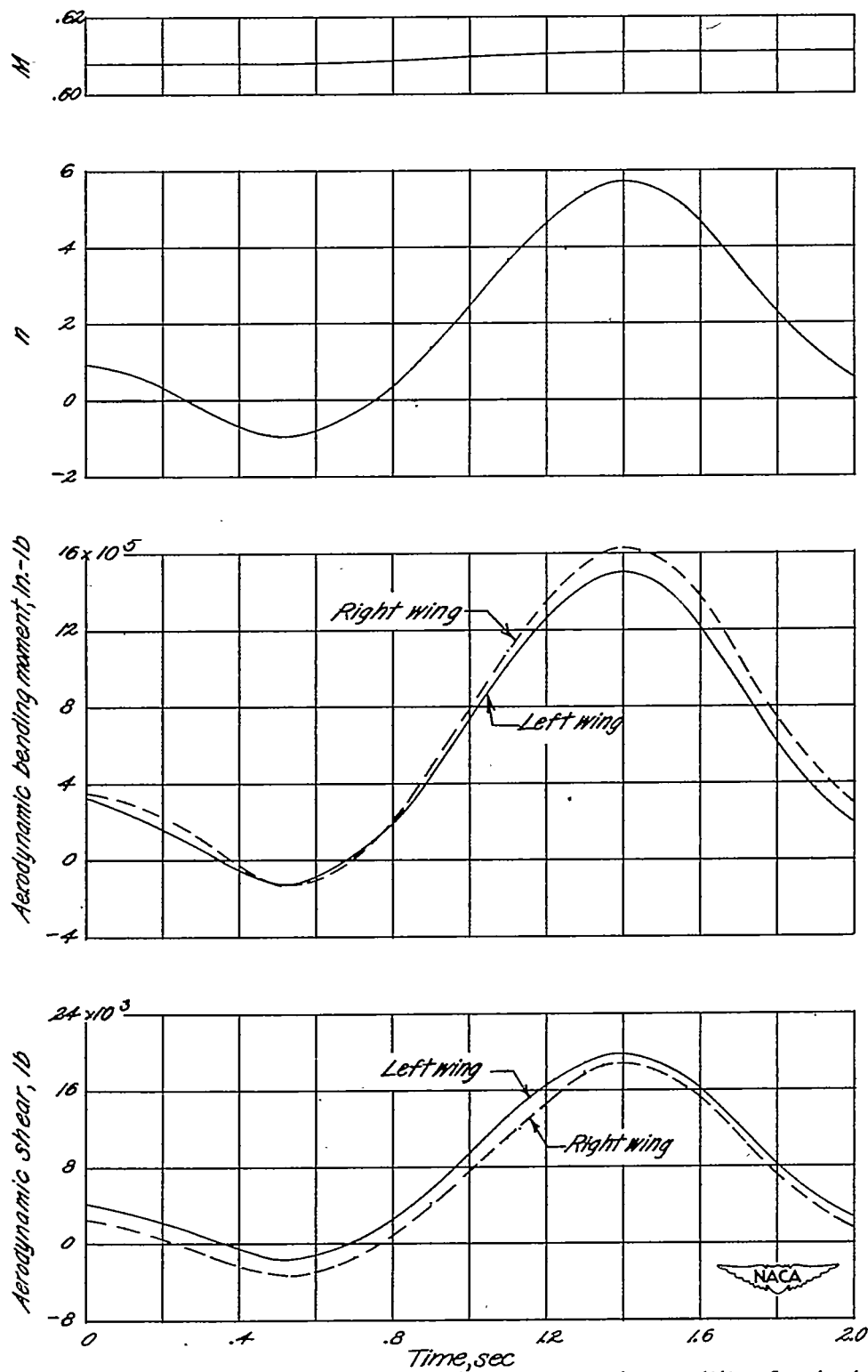
Figure 2.—Typical time histories of various measured quantities for test airplane in an abrupt push-down—pull-up maneuver. Pressure altitude, 10,000 feet.
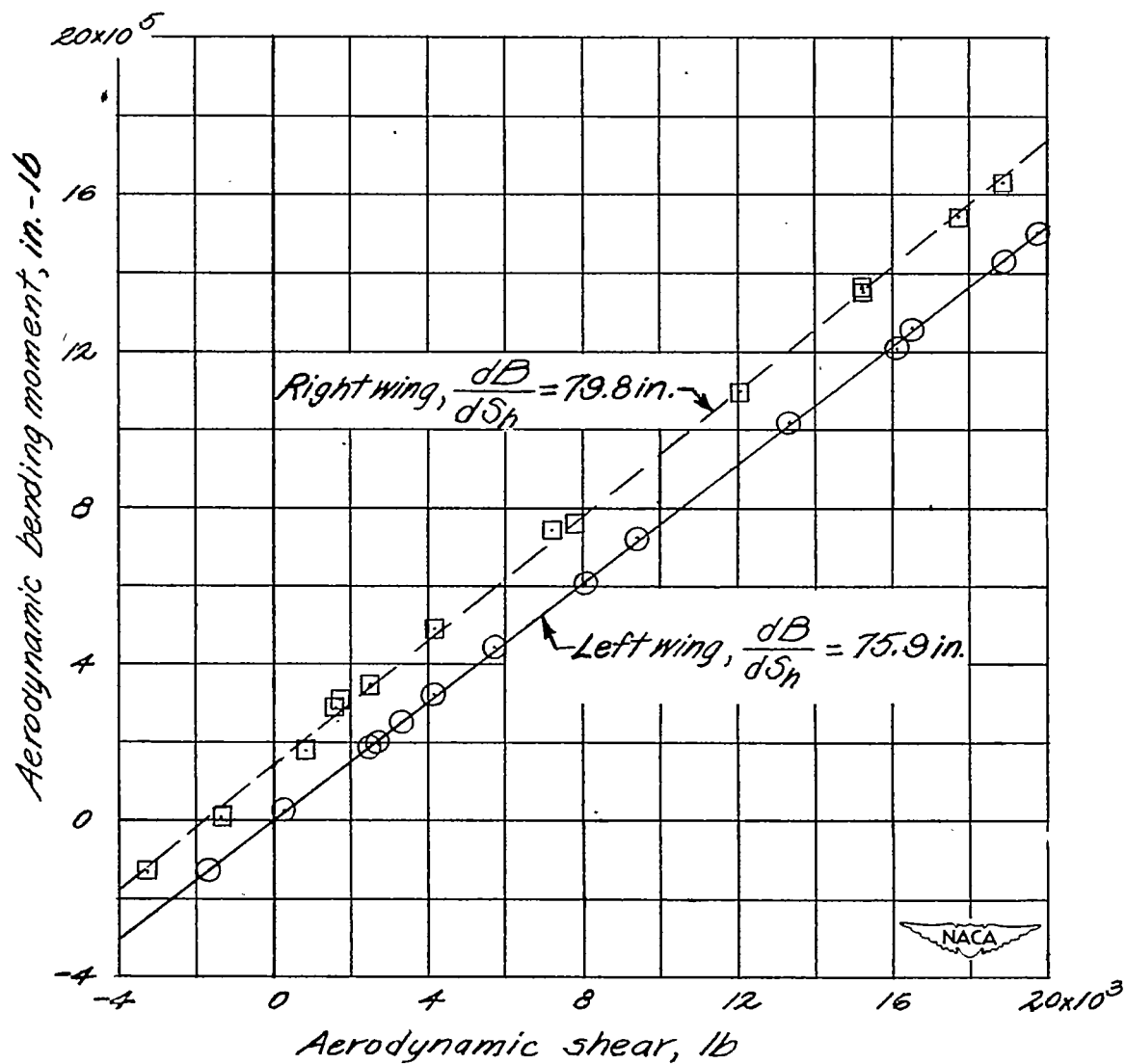
Figure 3.— Typical measured variation of aerodynamic
bending moment with aerodynamic shear
for left and right wings of test airplane
during manuever shown in figure 2. Mach
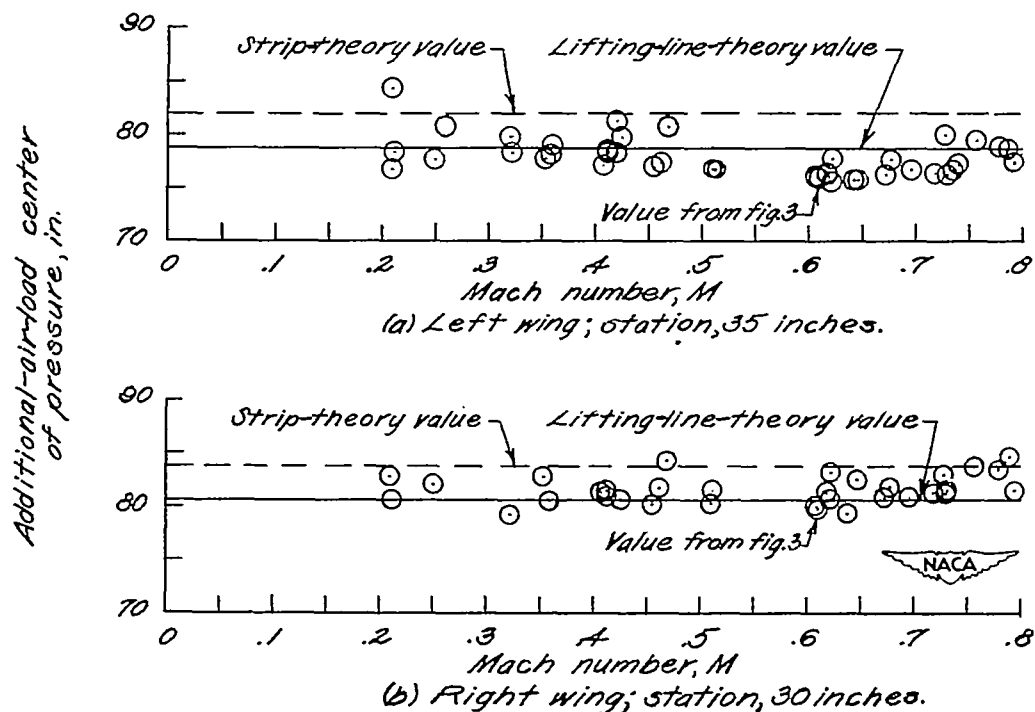number, 0.61; pressure altitude, 10,000 feet.

(a) Left wing; station, 35 inches.

(b) Right wing; station, 30 inches.

Figure 4. — Variation of left- and right-wing additional-air-load centers
of pressure with Mach number for test airplane as
determined from strain-gage measurements in flight.
The centers of pressure are for loads outboard of the
listed strain-gage stations.
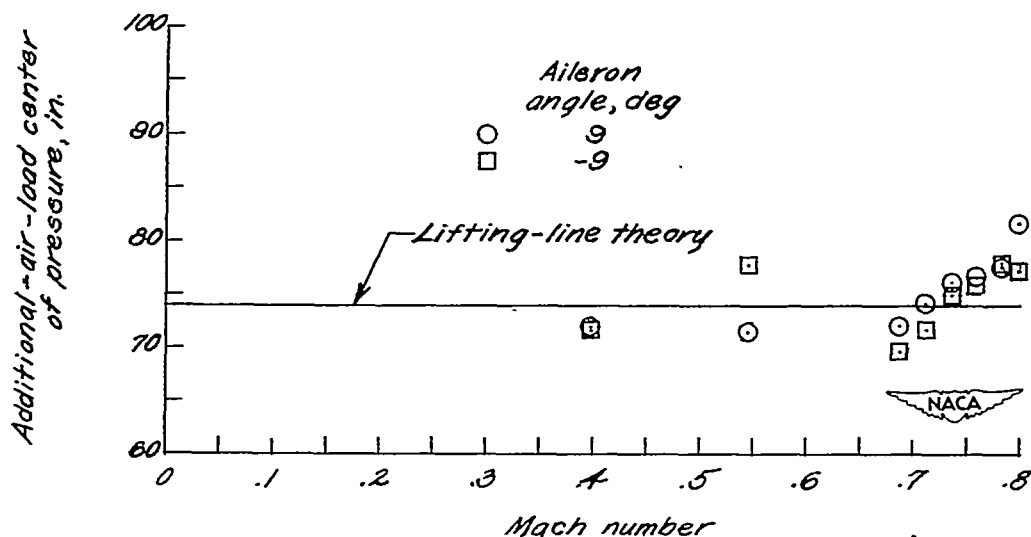
Figure 5. — Additional-air-load center of pressure outboard of wing
semispan station, $\frac{y}{b/2} = 0.215$, for $\frac{1}{3}$-scale model of prototype
of the test airplane. Data from Ames 16-foot high-speed
wind-tunnel pressure-distribution tests scaled to full size.

(a) Data from pressure-distribution measurements outboard of station $\frac{y}{b/2} = 0.118$ for airplane of reference 2.

(b) Data from pressure-distribution measurements outboard of station $\frac{y}{b/2} = 0.30$ for airplane of reference 3.
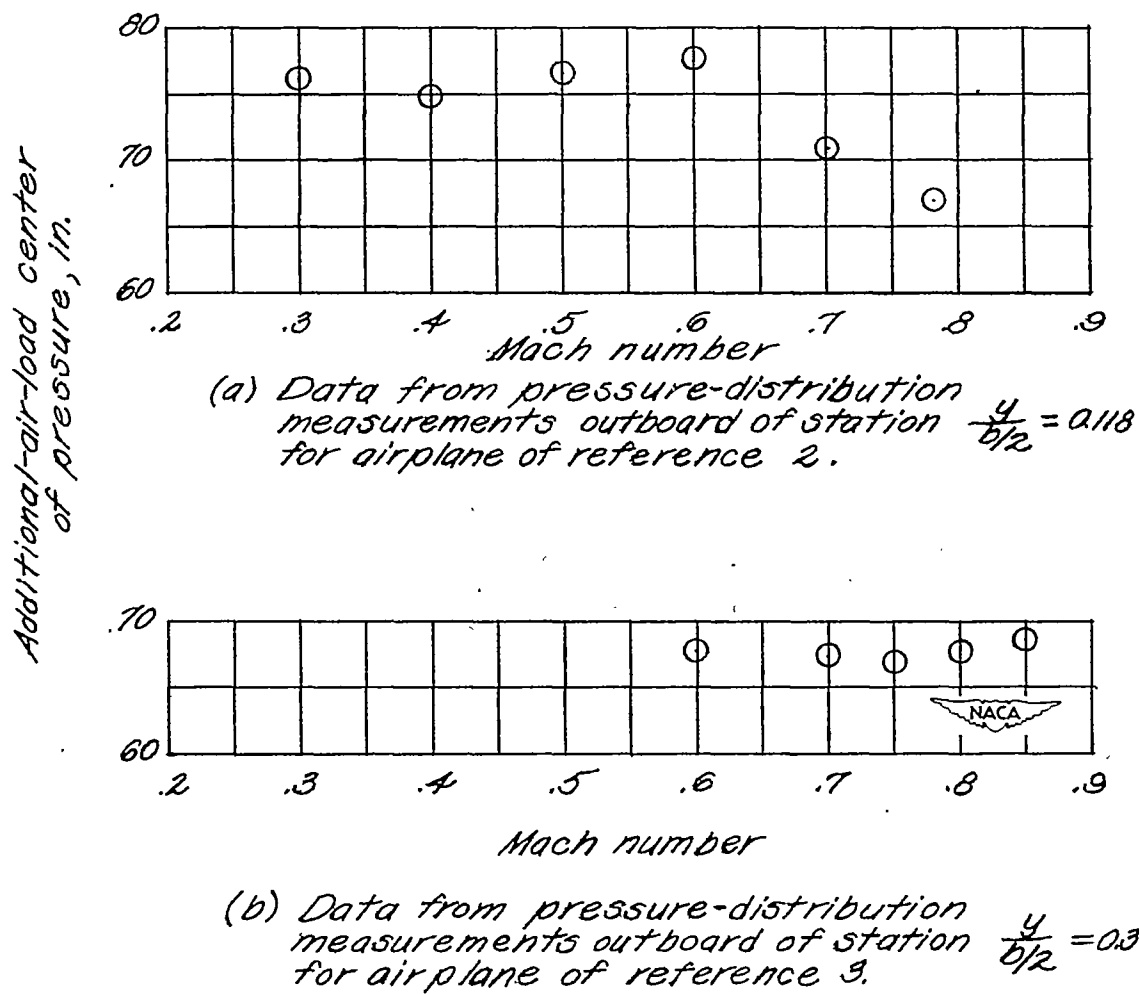
Figure 6.- Variation of the additional-air-load center of pressure from pressure-distribution measurements on two airplanes.
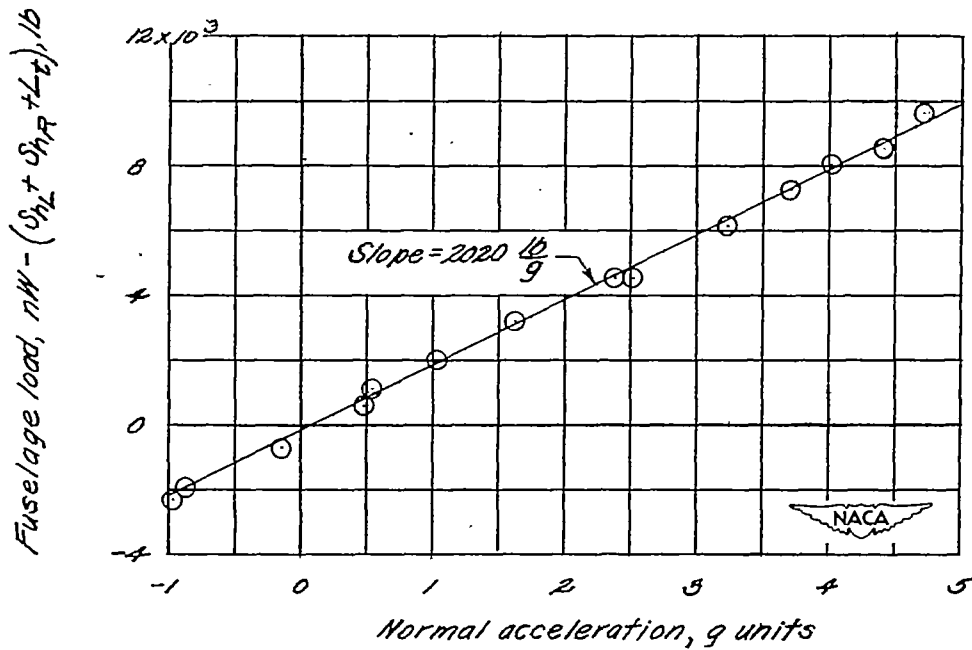
Figure 7.- Typical variation of fuselage load with normal acceleration for an abrupt push-down — pull-up maneuver of test airplane. Mach number, 0.51; pressure altitude, 20,000 feet.
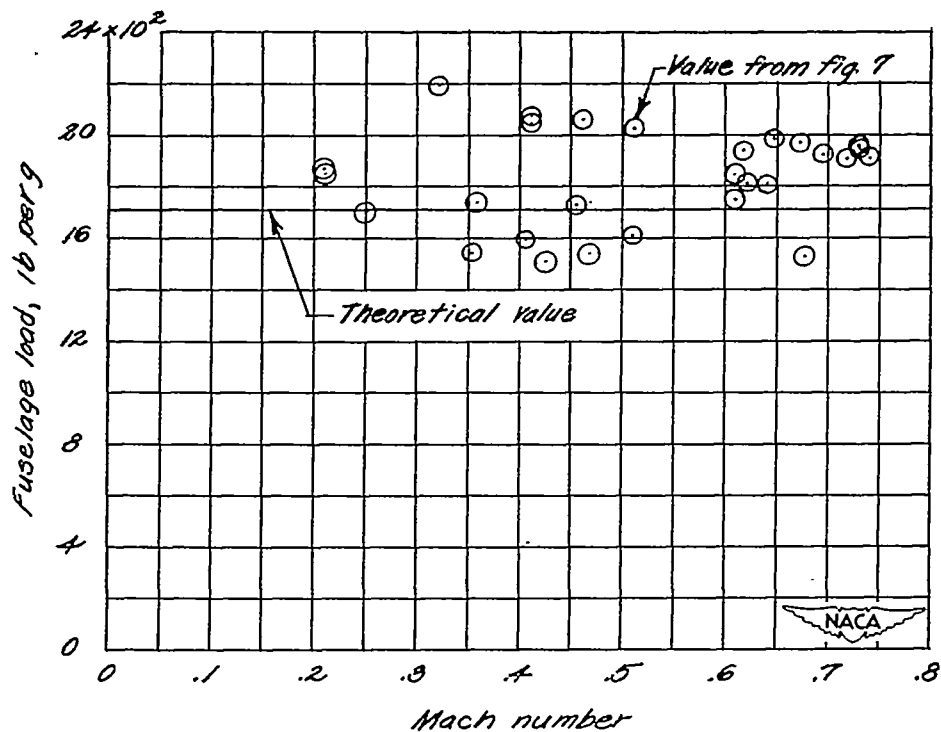
Figure 8.- Variation of fuselage load per unit normal acceleration with Mach number for test airplane.
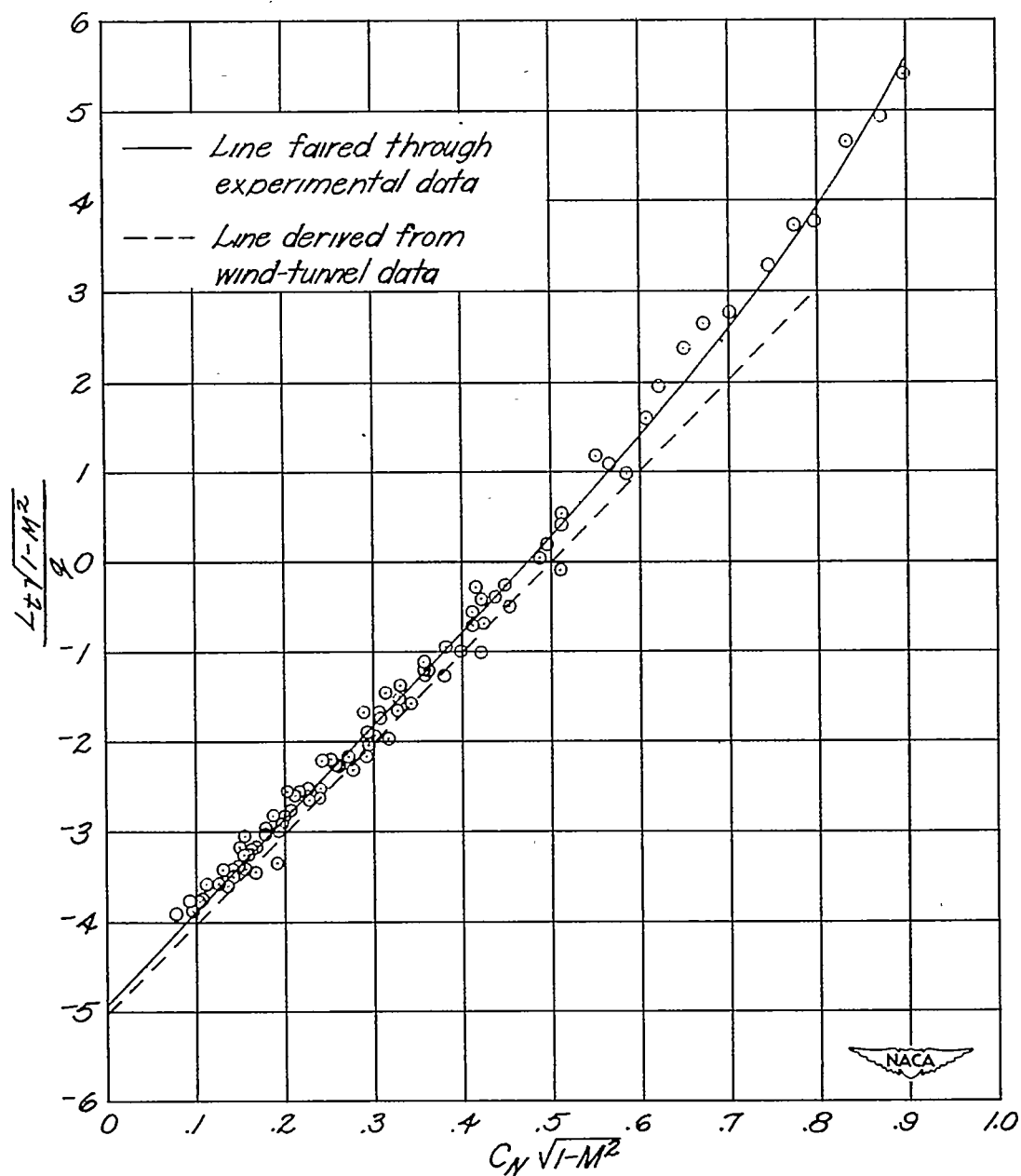
Figure 9.—Variation of tail-load parameter with airplane normal-force coefficient for test airplane. Airplane weight, 8750 pounds; center-of-gravity position, 25.1 percent mean aerodynamic chord.
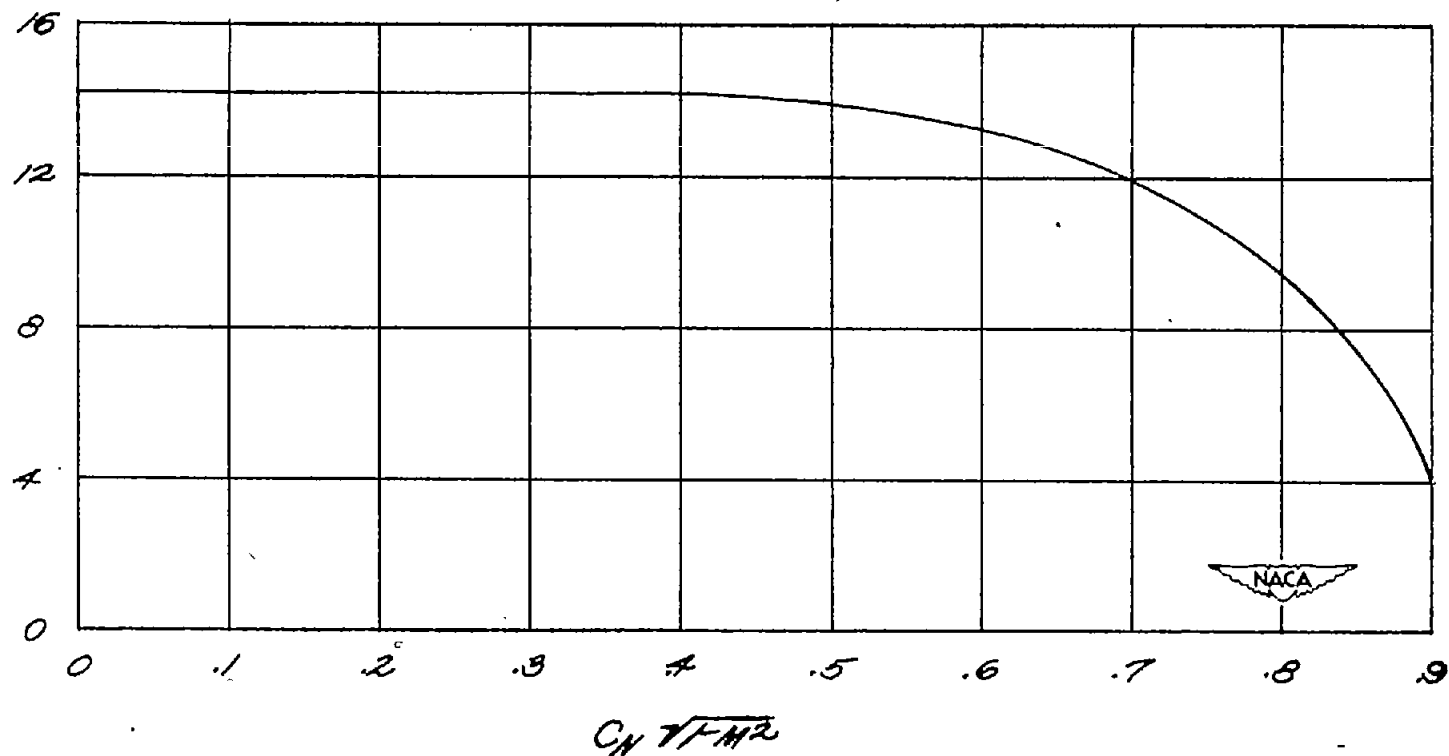
Figure 10.- Aerodynamic-center position for test airplane as a function of airplane normal-force coefficient.
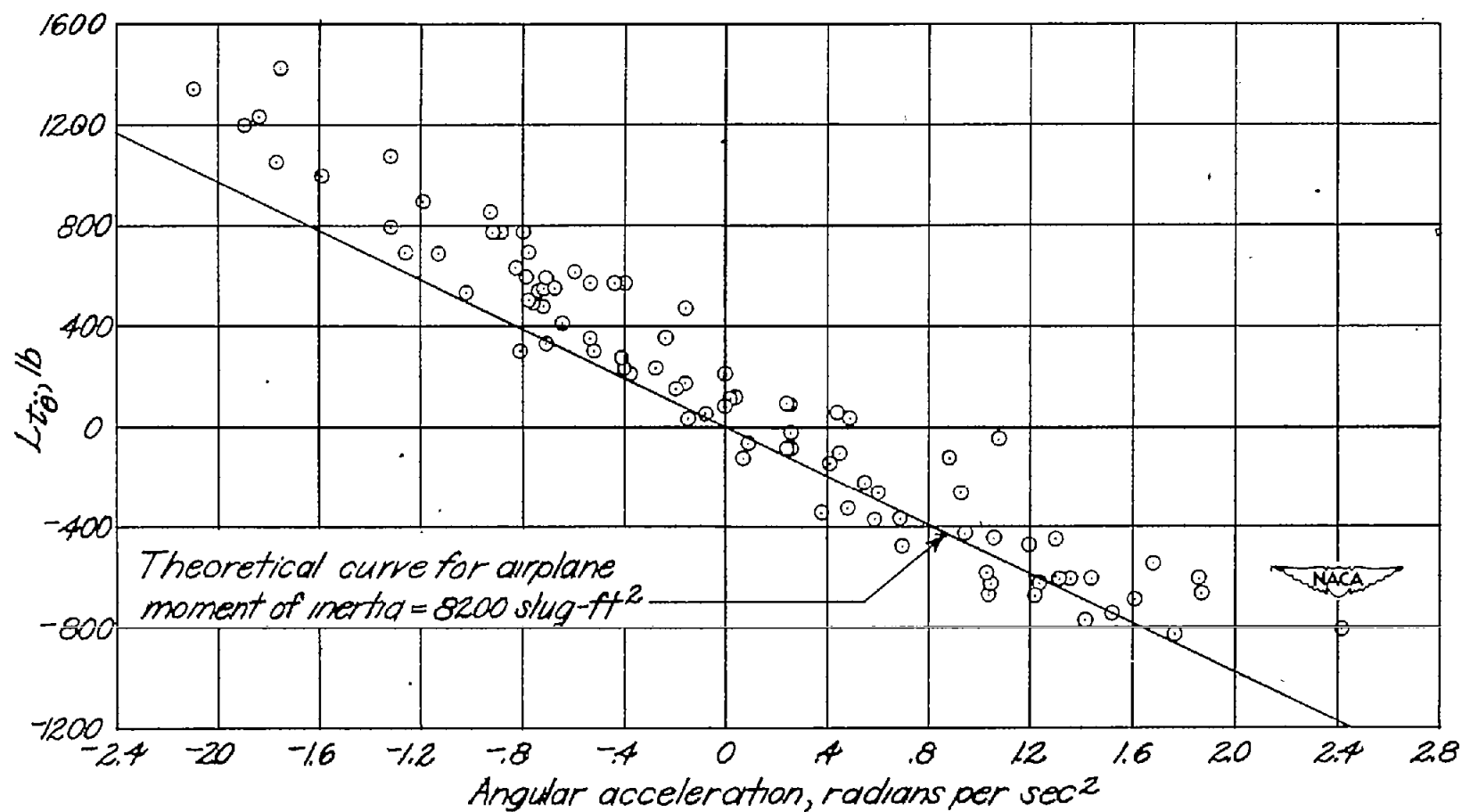
Figure 11.—Variation of angular-acceleration tail load with angular acceleration as determined from flight data for test airplane.